MIT Libraries | DSpace@MIT

MIT Open Access Articles

Collision kernels from velocity-selective optical pumping with magnetic depolarization

Massachusetts Institute of Technology

Collision kernels from velocity-selective optical pumping with magnetic depolarization

T. Bhamre,[1] R. Marsland III,[2] I. K. Kominis,[3] B. H. McGuyer,[1,*] and W. Happer[1]

[1]*Department of Physics, Princeton University, Princeton, New Jersey 08544, USA*
[2]*Department of Physics, Massachusetts Institute of Technology, Cambridge, Massachusetts 02139, USA*
[3]*Department of Physics, University of Crete, Heraklion 71103, Greece*

We experimentally demonstrate how magnetic depolarization of velocity-selective optical pumping can be used to single out the collisional cusp kernel best describing spin- and velocity-relaxing collisions between potassium atoms and low-pressure helium. The range of pressures and transverse fields used simulate the optical pumping regime pertinent to sodium guidestars employed in adaptive optics. We measure the precession of spin-velocity modes under the application of transverse magnetic fields, simulating the natural configuration of mesospheric sodium optical pumping in the geomagnetic field. We also provide a full theoretical account of the experimental data using the recently developed cusp kernels, which realistically quantify velocity damping collisions in this optical pumping regime. A single cusp kernel with a sharpness $s = 13 \pm 2$ provides a global fit to the K-He data.

PACS number(s): 32.80.Xx, 34.20.Cf, 05.60.Cd, 95.75.Qr

I. INTRODUCTION

We demonstrate an alternative way to measure the transition matrix $W(v,v')$ for velocity-changing collisions between ground-state alkali-metal atoms and arbitrary buffer-gas atoms or molecules in the classical limit. This matrix contains all of the information required for computing the contribution of collisions to the evolution of nonequilibrium velocity distributions in the vapor, which can be written as a Master equation

$$\frac{\partial p(v,t)}{\partial t} = -\gamma_{\text{vd}} p(v,t) + \gamma_{\text{vd}} \int dv' W(v,v') p(v',t), \quad (1)$$

where $p(v,t)$ is the time-dependent velocity distribution and γ_{vd} is the rate of velocity-changing collisions. Precise measurements of this matrix have long been of interest as a way to place empirical constraints on the interatomic potential for alkali-metal–buffer-gas pairs [1]. Two new applications demand an increasingly precise knowledge of $W(v,v')$. First of all, the ease with which nonequilibrium velocity distributions can be created through velocity-selective optical pumping makes alkali-metal vapor cells an ideal candidate for investigating new theorems of nonequilibrium statistical mechanics (reviewed in [2]). $W(v,v')$ is the transition probability that arises in Markov derivations of these theorems, and quantitative knowledge of its behavior for real systems would make such experiments easier to design and analyze. Second, laser guidestars employed in the adaptive optics systems of modern terrestrial observatories produce nonequilibrium velocity distributions of optically pumped mesospheric sodium atoms. The numerical models used for optimizing the laser parameters for maximum backscatter require $W(v,v')$ as input, but the dearth of empirical measurements for sodium-air collisions has forced current models to use a highly simplified model, where $W(v,v')$ is the Boltzmann distribution in v independent of v' [3]. In Sec. II we present the theory behind

our measurement, while in Sec. III we discuss the experiment and data analysis.

II. THEORY

The theoretical framework we employed to design the experiment and analyze our data is laid out in detail in [4]. Here we summarize the points that are most directly relevant to the current work.

We model the vapor cell as an ensemble of single atoms whose velocities are perturbed by collisions with atoms of an inert buffer gas and with the cell walls. Since radiation-pressure effects relevant to laser cooling experiments are negligible at the high temperatures that we are interested in, the equilibrium velocity distribution of atoms in the buffer gas remains the Maxwell-Boltzmann distribution even in the presence of laser light. It will be convenient to measure atomic velocities in units of the most probable speed, $v_D = \sqrt{2k_B T/M}$, where T is the temperature of the cell and M is the mass of the atom. We will denote the projection v of the atomic velocity onto the laser beam direction by $x = v/v_D$. Although the overall velocity distribution remains constant, the incident laser beam introduces correlations between the spins and the velocities: due to the Doppler shift, a laser at frequency ω excites a resonance at frequency ω_0 only in atoms with velocity $x_0 = (\omega - \omega_0)/k v_D$ along the beam. This is the origin of "velocity-selective optical pumping" (VSOP), whereby the distribution of atomic spin states becomes velocity dependent. We assume the laser is weak enough that the small fraction of atoms in the excited states at any given time can be ignored, so the effect of the laser is to modify the distribution of ground-state sublevels at the resonant velocities. The distribution among energy sublevels $|\mu\rangle$ for atoms with velocities between x and $x + dx$ is described by the $(2I + 1)(2S + 1) \times (2I + 1)(2S + 1)$ density matrix $d\rho(x)dx = \sum_{\mu\nu} \chi_{\mu\nu}(x)|\mu\rangle\langle\nu|\,dx$, where S and I are the electron and nuclear spin quantum numbers, respectively, and $|\mu\rangle$ and $|\nu\rangle$ are eigenstates of the ground-state Hamiltonian with eigenvalues E_μ and E_ν, respectively. The ground-state Hamiltonian includes hyperfine splitting and Zeeman coupling to an external magnetic field. $\chi_{\mu\nu}(x)$ are the

---
*Present address: Department of Physics, Columbia University, 538 West 120th Street, New York, New York 10027-5255, USA.
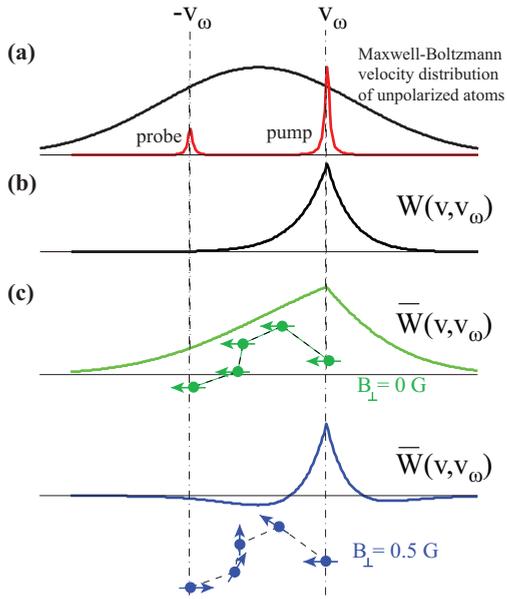
FIG. 1. (Color online) (a) The monochromatic, circularly polarized pump laser of frequency ω selectively spin polarizes atoms in the velocity group around v_ω that is Doppler shifted into resonance. The counterpropagating probe beam of the same laser probes atoms at the velocity group around $-v_\omega$. Pumped atoms collide with buffer-gas atoms, and each collision transfers atoms from velocity v to velocity v' with probability $W(v,v')$, shown in (b) for $v' = v_\omega$. (c) To the first order in pump intensity, the overall effect of all the collisions is to add a broad "pedestal" given by $\overline{W}(v,v_\omega)$ to the sharply peaked distribution of average spin as a function of velocity. Since the absorption of the circularly polarized probe beam depends on the atomic spin, scanning the laser frequency provides a measurement of $\overline{W}(-v_\omega,v_\omega)$. (d) A transverse magnetic field causes the spins to precess as the atoms diffuse through velocity space, providing a precise "clock" that helps constrain estimates of the damping rates required to analyze the data. The effect of this spin precession is clearly seen in the sign reversal of $\overline{W}(-v_\omega,v_\omega)$ at $B_\perp = 0.5$ G relative to the value at 0 G.

velocity-dependent amplitudes of the density-matrix elements $|\mu\rangle\langle\nu|$.

In a VSOP situation with no velocity-changing collisions, some of the density-matrix elements will have amplitudes $\chi_{\mu\nu}(x)$ sharply peaked around the resonant velocities x_0. As illustrated in Fig. 1, adding an inert buffer gas allows atoms pumped at the resonant velocities to jump to other, nonresonant velocities through collisions with the buffer gas that change the atomic velocity while preserving spin polarization. Figure 1 also displays the effect of a transverse magnetic field, which causes Larmor precession of the spins while the atom diffuses from the pump resonant velocity to the probe resonant velocity, thus adding a new tunable time scale to the problem.

The velocity-changing collisions are characterized by the "collision kernel" $W(x,x')$, which gives the probability that an atom with initial velocity x' will have velocity x after a single collision. Since our atoms remain in the spherically symmetric $l = 0$ state of orbital angular momentum for the overwhelming majority of the time, the collision kernel is independent of the internal atomic state. The overall effect of collisions is to give $\chi_{\mu\nu}(x)$ a broad pedestal around the sharp resonant spike, and

the shape of this pedestal contains valuable information about the collision kernel. To extract this information, we need to first write the steady-state solutions to the evolution equation for the $\chi_{\mu\nu}$'s in terms of $W(x,x')$, and then find a good ansatz form for $W(x,x')$ that can reproduce experimental data through the appropriate adjustment of a few free parameters.

The evolution of the velocity distribution $\chi_{\mu\nu}(x)$ of density-matrix element $|\mu\rangle\langle\nu|$ is described by

$$\frac{\partial \chi_{\mu\nu}(x,t)}{\partial t} = -\int K_{\mu\nu}(x,x')\chi_{\mu\nu}(x',t)dx' + P_{\mu\nu}(x), \quad (2)$$

where the damping kernel is

$$K_{\mu\nu}(x,x') = [\gamma_{\mathrm{w}} + i\Omega_{\mu\nu} + \gamma_{\mathrm{vd}}]\delta(x - x') - \gamma_{\mathrm{vd}}W(x,x'). \quad (3)$$

The rate of loss of polarized atoms due to diffusion or free flight to the walls is γ_{w}. The Bohr frequencies $\Omega_{\mu\nu} = (E_\mu - E_\nu)/\hbar$ depend on the applied magnetic field. For laboratory experiments with alkali-metal atoms in low buffer-gas pressures, the direct damping of spin polarization by gas-phase collisions can be neglected, since practical buffer gases like N_2 or the noble gases He, Ne, Ar, etc. have such small spin-flip rates compared to γ_{w}. The main effect of the buffer gas on spin relaxation is to lengthen the time needed for a polarized atom to diffuse to the wall, that is, to decrease γ_{w}. The rate of velocity relaxation due to the buffer gas is parametrized by the rate γ_{vd} at which atoms with initial velocity x' are transferred to a range of final velocities x.

The laser-atom interaction that creates the nonequilibrium distribution of optically pumped atoms enters the model through the source term $P_{\mu\nu} = P_{\mu\nu}(x,\chi_{\mu'\nu'})$, which depends on the values $\chi_{\mu'\nu'}(x)$ of all the density-matrix element amplitudes at velocity x. For a true monochromatic light source exciting electrons to states with infinite lifetimes, $P_{\mu\nu}$ would be a superposition of δ functions. In fact, the finite excited-state lifetime, finite laser linewidth, and other experimental issues combine to produce a Lorentzian source term with a particular width, which can be empirically determined from a measurement without buffer gas.

The nonequilibrium steady-state velocity distribution of the density-matrix element $|\mu\rangle\langle\nu|$ is found by setting $\partial\chi_{\mu\nu}/\partial t = 0$ in Eq. (2), and is formally given by

$$\chi_{\mu\nu}(x) = \int K_{\mu\nu}^{-1}(x,x')P_{\mu\nu}(x')dx', \quad (4)$$

where the inverse damping kernel is defined by $\int K_{\mu\nu}^{-1}(x,x')K_{\mu\nu}(x',x'')dx' = \delta(x - x'')$. Note that $P_{\mu\nu}$ depends on the $\chi_{\mu\nu}$'s, so this is not a closed-form solution, but we can use it to obtain a power-series solution in the pump-laser intensity, as shown explicitly in Eqs. (134) through (136) of [4]. Our numerical calculations use the first-order solution, given by Eqs. (137) through (140) of [4].

We now need a physically reasonable and computationally tractable ansatz for $W(x,x')$ in order to extract information about the collisions from experimental signals. McGuyer *et al.* have shown that "cusp kernels" $C_s(x,x')$ meet these requirements [5]. The cusp kernel function has a single free parameter s called the "sharpness", which we will employ as a fit parameter to match our model predictions to our experimental data. Under the assumption that the collision kernel can be

modeled by a single cusp kernel, $W(x,x') = C_s(x,x')$, the inverse damping kernel $K_{\mu\nu}^{-1}$ takes on the particularly simple form [5]

$$K_{\mu\nu}^{-1}(x,x') = \frac{1}{\gamma_w + i\Omega_{\mu\nu} + \gamma_{vd}}$$

$$\times \left[\delta(x - x') + \frac{\gamma_{vd}}{\gamma_w + i\Omega_{\mu\nu}} C_{r_{\mu\nu}}(x,x') \right]. \quad (5)$$

That is, the inverse kernel is the sum of a δ-function and another cusp kernel with modified sharpness $r_{\mu\nu}$ given by

$$r_{\mu\nu} = \frac{\gamma_w + i\Omega_{\mu\nu}}{\gamma_w + i\Omega_{\mu\nu} + \gamma_{vd}} s. \quad (6)$$

The δ-function part comes from atoms that have not had collisions with the buffer gas, and the cusp kernel part contains the net result of all the buffer-gas collisions that take place over the lifetime of a spin-polarized atom. In [4] and in our Fig. 1, we represent this "pedestal" term that contains the collision information by the symbol $\bar{W}(x,x')$.

Using this result and Eq. (4), we can obtain the steady-state $\chi_{\mu\nu}$'s in terms of the atomic parameters γ_w, γ_{vd}, and s. The rates γ_w and γ_{vd} can be determined experimentally, so the solution has s as its only free parameter. Once we calculate the probe beam absorption spectrum from the $\chi_{\mu\nu}$'s, we can easily find the sharpness s that gives a least-squares best fit to the data.

The experiment we performed is similar to the experiment of Aminoff *et al.* [6], with the main difference being our addition of magnetic depolarization via Larmor precession around a transverse magnetic field. The authors in [6] noted that the traditionally used Keilson-Storer kernel was a poor approximation of the actual kernel, since it could not fit the data over a broad range of pressures and the kernel's parameter was thus not unique but pressure dependent. In contrast, we will demonstrate that a cusp kernel with a single sharpness can provide a global fit to the data. The additional, experimentally controllable parameter of the transverse magnetic field, incorporated in our formalism through the frequencies $\Omega_{\mu\nu}$, provides a systematic check of our understanding of the kernel [7–11].

III. EXPERIMENT AND DATA ANALYSIS

Figure 2 schematically depicts our apparatus. We inserted one of three cylindrical sealed glass cells containing potassium and helium buffer gas at three different pressures into the path of two counterpropagating circularly polarized beams from a Toptica DL Pro tunable diode laser. The pump beam produces the spin-velocity correlations, which are measured by the much weaker probe beam. To amplify the signal, we modulated the circular polarization of the probe beam with a photoelastic modulator (PEM), cycling the polarization from right circular to left circular and back at a frequency of 42 kHz. Since the potassium vapor transmits both polarizations with the same efficiency in the absence of optical pumping, we were able to isolate and amplify the effect of optical pumping on the transmission efficiency of the probe beam with a lock-in amplifier phase locked to the PEM, while slowly scanning the laser frequency over the potassium's Doppler profile.
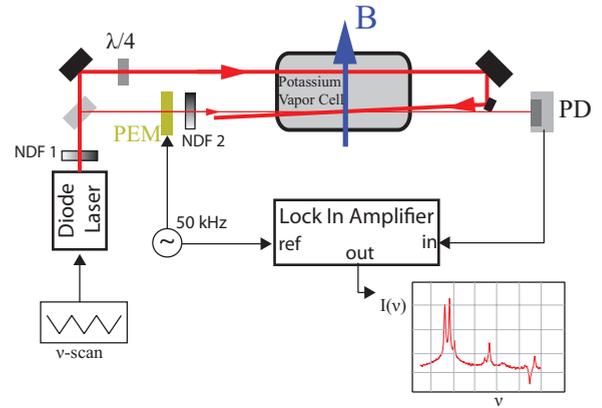

FIG. 2. (Color online) Counterpropagating pump-probe lasers create and probe nonequilibrium spin-velocity distributions of potassium vapor in helium buffer gas. The atoms are contained in sealed glass cells of 1/2 in diameter and 5/4 in length, residing in an oven air heated at 69 ± 0.2 °C to maintain a high enough potassium vapor pressure of natural isotopic abundance, 93.26% ^{39}K and 6.73% ^{41}K. The cell and oven reside in the middle of three pairs of Helmholtz coils along three mutually orthogonal axes providing a homogeneous, constant, and tunable magnetic field. The intensities of the two counterpropagating beams were independently controlled with two neutral density filters. An angular separation of less than 5 mrad was introduced between the beams to avoid blockage of the probe detection photodiode by the pump mirror.

Since the pump beam only pumps atoms having velocities $x_{\mu\bar{\nu}} = (\omega - \omega_{\mu\bar{\nu}})/kv_D$, where $\omega_{\mu\bar{\nu}}$ is the frequency of the transition from ground-state sublevel μ to excited-state sublevel $\bar{\nu}$, and the probe beam only interacts with atoms with opposite velocities $-x_{\mu\bar{\nu}}$, the spectrum of probe beam transmission will display sharp saturated-absorption spikes at $\omega_{\mu\bar{\nu}}$ as well as the crossover lines $(\omega_{\mu\bar{\nu}} + \omega_{\mu'\bar{\nu}'})/2$, where the pump and probe beams can simultaneously interact with the same atoms. As discussed above, the velocity-changing collisions superimpose a broad pedestal on these spikes, which contains the desired information about the kernel $W(x,x')$. To ensure that the probe beam does not modify the atomic density matrix, we measured the height of the tallest spike at various probe intensities and a constant pump intensity, by adjusting filter NDF2 in Fig. 2. At low probe intensities, the height scales linearly with intensity, while it becomes quadratic as the probe beam begins to modify the spin polarization. We observed that a ratio of probe-to-pump intensity of about 10% was well within the linear regime, so we set NDF2 to the corresponding attenuation. Similarly, we confirmed that we could safely neglect the second- and higher-order terms in pump beam intensity from the series solution of Eq. (4) by examining the resonance's scaling with pump intensity and staying within the linear regime. As indicated in Fig. 2, the filter (NDF1) for adjusting the pump intensity was positioned before the beam splitter, so that we could adjust the pump intensity at a constant probe/pump intensity ratio. In the first-order regime, the transmitted intensity should scale linearly with each beam intensity individually, and so their simultaneous variation should produce a quadratic shape. We set NDF1 so that we are well within this quadratic regime.
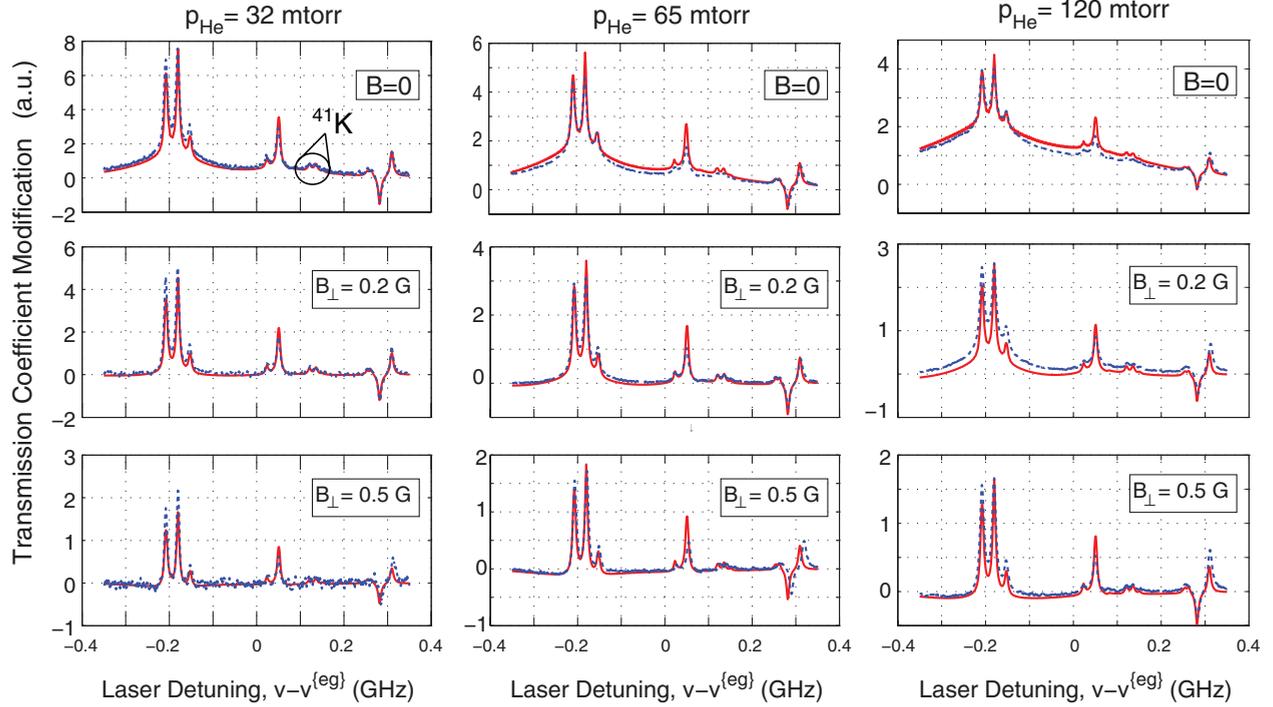
FIG. 3. (Color online) Potassium-helium data. Shown is the measured (red lines) and calculated (blue, dashed lines) absorption rate of the probe beam for three different magnetic fields (zero field, 0.2 G, and 0.5 G, transverse to the laser propagation direction) at pressures of 32, 65, and 120 mTorr. The theoretical rates were calculated assuming that the velocity-changing collisions are well modeled by a single cusp kernel, with the sharpness $s = 13$ determined by a least-squares best fit to all the data.

In Fig. 3, we show the data acquired from our three cells at three different transverse magnetic fields for each cell, along with the theoretical fits. To compare the measured line shapes to the cusp kernel predictions, we used Eqs. (143) through (147) of [4] to obtain the first-order line-shape corrections from the spin mode amplitudes $\chi_{\mu\nu}$. The required rates γ_{vd} and γ_{w} were obtained from the expressions

$$\gamma_{\text{vd}} = \frac{v_D^2}{2D}(s+1) \tag{7}$$

and

$$\frac{1}{\gamma_{\text{w}}} = \frac{a}{v_D} + \frac{a^2}{8D}\left[1 + 4\ln\left(\frac{b}{a}\right)\right], \tag{8}$$

given in Eqs. (A1) and (79) of [4], respectively. The most probable speed v_D and the sharpness parameter s have already been defined. The laser beam and cell radii are $a = 0.06$ cm and $b = 0.56$ cm, respectively, and D is the diffusion coefficient of potassium atoms in helium, inversely proportional to the helium pressure. We used the value $D_0 = 0.45$ cm^2/s for 1 atm of helium. Equation (7) relating γ_{vd} to the diffusion coefficient D is a special case of a relation introduced by Berman *et al.* for reducing the number of free parameters in VSOP collision kernel measurements [12].

To correct for potassium's optical thickness, leading to pump and probe intensity variation along the length of the cell, we divide the data by the factor

$$f(\omega) = \frac{e^{-\sigma(\omega)nl}}{\sigma(\omega)}(1 - e^{-\sigma(\omega)nl}), \tag{9}$$

where $\sigma(\omega)$ is the absorption cross section of the unpolarized potassium atoms, n is the number density of potassium atoms (a known function of temperature [13]), and $l = 2.7$ cm is the length of the cell.

We also had to account for the fact that our pressure gauge had a large uncertainty at the low pressures we were using. To get a good fit, we had to adjust the pressure values input to the model within the range of uncertainty, and ultimately use the values 32, 65, and 120 mTorr instead of the nominal 25, 50, and 100. Finally, we added one more free parameter to match the absolute scale of the y axis in Fig. 3 between model and data. We used the same scale factor for all nine data traces in Fig. 3. The simultaneous least-squares fit of the model to the nine data traces is superimposed on the data in Fig. 3, resulting in a sharpness of $s = 13 \pm 2$.

IV. CONCLUSIONS

In conclusion, we have demonstrated a simple way to accurately determine the sharpness of cusp kernels modeling velocity-selective optical pumping. In particular, we have shown that a single cusp kernel is sufficient to reproduce line-shape measurements far from the Maxwell-Boltzmann equilibrium, across a variety of pressures and magnetic fields. The employed method of magnetic depolarization allows a rapid, experimentally straightforward and accurate measurement of collision kernels useful for constraining interatomic potentials, testing nonequilibrium statistical mechanics theorems, or optimizing laser guidestar systems.

[1] K. E. Gibble and J. Cooper, Phys. Rev. A **44**, R5335 (1991).

[2] C. Jarzynski, Annu. Rev. Condens. Matter Phys. **2**, 329 (2011).

[3] S. M. Rochester *et al*., J. Opt. Soc. Am. **29**, 8 (2012).

[4] R. Marsland III, B. H. McGuyer, B. A. Olsen, and W. Happer, Phys. Rev. A **86**, 023404 (2012).

[5] B. H. McGuyer, R. Marsland III, B. A. Olsen, and W. Happer, Phys. Rev. Lett. **108**, 183202 (2012).

[6] C. G. Aminoff, J. Javanainen, and M. Kaivola, Phys. Rev. A **28**, 772 (1983).

[7] W. Happer, G. J. MacDonald, C. E. Max, and F. J. Dyson, J. Opt. Soc. Am. **11**, 263 (1994).

[8] W. Happer, Y-Y. Jau, and T. G. Walker, *Optically Pumped Atoms* (Wiley-VCH Verlag/GmbH, Weinheim, 2010).

[9] M. A. Bouchiat, J. Phys. France **24**, 379 (1963).

[10] J. Keilson and J. E. Storer, Q. Appl. Math **10**, 243 (1952).

[11] S. W. Morgan and W. Happer, Phys. Rev. A **81**, 042703 (2010).

[12] P. R. Berman, J. E. M. Haverkort, and J. P. Woerdman, Phys. Rev. A **34**, 4647 (1986).

[13] C. Yaws, *Handbook of Vapor Pressure: Volume 4* (Gulf Professional, Houston, Texas, 1995).